Electrical Power and Energy Systems 123 (2020) 106219

Contents lists available at ScienceDirect

Electrical Power and Energy Systems

journal homepage: www.elsevier.com/locate/ijepes

Coordinated deliverable energy flexibility and regulation capacity of distribution networks

K. Oikonomou, M. Parvania*, R. Khatami

Department of Electrical and Computer Engineering, The University of Utah, Salt Lake City, UT 84112, United States

ARTICLE INFO

Keywords:
Distributed flexibility
Energy and regulation flexibility capacity

ABSTRACT

The increasing capacity of distributed flexibility resources (DFRs) in power distribution systems provides an unprecedented opportunity for distribution system operators (DSOs) to offer the available distributed flexibility as services in electricity markets. This paper proposes a novel model to define and co-optimize the deliverable energy flexibility and frequency regulation capacity of power distribution systems. The distributed flexibility is provided in distribution buses by flexible loads, modeled by a novel queuing system, energy storage (ES) devices, and distributed solar resources with controllable inverters. The proposed model co-optimizes the DFRs schedule in three operating points that model the operation of flexible loads, distributed solar generation units, and ES devices in distribution networks for providing energy flexibility, as well as regulation up and down capacity in electricity markets. The proposed model takes into account the interdependence between DFRs schedule in the three operating points, which enables the DSO to provide non-conflicting capacity offers to different services in the market. In addition, the proposed model ensures the deliverability of energy flexibility and regulation capacity in the markets by satisfying the power flow constraints of distribution networks in all three operating points. The numerical studies, conducted on the 33-bus test distribution system, demonstrate the effectiveness of the proposed model for scheduling realistic energy flexibility and regulation capacity offers that are deliverable in the markets.

1. Introduction

The proliferation of distributed flexibility resources (DFRs), including flexible loads, energy storage (ES) devices, and renewable resources with controllable inverters, together with current advancements in telecommunication infrastructure and automated control schemes create new opportunities to enhance power systems flexibility. This flexibility, if properly managed, can offer a range of services (e.g., flexible energy, congestion management, frequency regulation) to the independent system operators (ISOs), who operate bulk power systems, and help them counterbalance the variability and uncertainty of renewable generation resources [1–3]. Further, the provision of flexibility services could create a new source of revenue for distribution system operators (DSOs) who would offer the distributed flexibility in the wholesale electricity markets and compete with resources connected to the transmission grid [4,5].

Despite the attractiveness of utilizing DFRs to provide flexibility services to transmission systems, the main challenge for DSOs is to capture the full operational flexibility of a diverse portfolio of DFRs with different operation characteristics, and provide adequate conditions for market access without violating the operational constraints of distribution systems. Therefore, in order to exploit the potential flexibility of DFRs in power systems operation, DSOs must ensure the deliverability of services in electricity markets, and coordinate the information flow between DSOs and ISOs. This coordination would require advanced distribution network management schemes that optimize the power exchange at the DSO/ISO interface, and facilitate DSOs' participation in electricity markets [6].

The technical literature includes models that control DFRs operation for offering services in the markets. A model proposed in [7] schedules and aggregates distributed flexible loads, energy generation resources, and ES devices to offer as demand response in the day-ahead energy market, while a model in [8] optimizes the real and reactive power output of controllable solar inverters, ES devices, and plug-in electric vehicles (PEVs) to provide regulation services to bulk power systems. A market participation model is proposed in [9] to maximize the profits of a combined distributed wind-energy storage system in the day-ahead energy and regulation markets. A model that optimally schedules small wind farms for providing congestion management in distribution networks is developed in [10], while the aggregate flexibility from flexible

* Corresponding author.
E-mail address: masood.parvania@utah.edu (M. Parvania).

https://doi.org/10.1016/j.ijepes.2020.106219
Received 21 December 2019; Received in revised form 18 May 2020; Accepted 23 May 2020

loads is deemed as a transmission level congestion relief measure in [11]. Models that aim to optimize the participation of PEVs in the energy and regulation markets via controlling their charge and discharge schedules have been studied in [12–15]. A stochastic model that schedules the regulation capacity of PEVs considering a performance-based compensation scheme and the uncertainty of the ISO's regulation signal is proposed in [16]. In [17], a smart building operator aggregates building flexible loads for providing regulation services to the ISO, while in [18] thermostatically controlled loads (TLCs) from air-conditioning systems are utilized to offer their aggregate flexibility to the frequency regulation markets, considering residents' thermal comfort. A Volt/Var control scheme is proposed in [19] for optimizing the reactive power dispatch of solar inverters in order to minimize distribution lines' losses and maximize solar penetration. In [20], an optimal solar inverter dispatch framework that enables both reactive and active controllability and maintains the inverter power factor above a prescribed value to secure its compliance with power quality standards is proposed to facilitate high solar penetration in power distribution networks.

In addition, multiple research works have investigated the operational flexibility of power distribution systems [21]. In [22], the concept of flexible operation region (FOR) is presented to determine the admissible region in the P-Q plane formed by active and reactive power flows at the distribution system. More specifically, a set of random control scenarios is generated and the boundaries of FOR are sketched such that the state variables of the distribution system could change within the operational constraints. A similar logic is used in [23], where a parametric linear combination of active and reactive power flows is optimized through an iterative process. The works in [22,23] neglect the market-based features of flexibility reserve scheduling and provide abstract not detailed models for DFRs. In [24], an optimization framework is introduced to counterbalance the inherent uncertainties of distributed renewable energy resources by controlling the nodal flexibility and lines' loadability in power distribution systems. In [25], the DSOs reserve procurement is formulated through a three-stage stochastic model. The works in [24,25] schedule and deploy the flexibility within distribution networks, however, without considering the flexibility offered by distribution systems to the transmission network. The deliverable energy flexibility of distribution systems is defined and optimized in [26] as the aggregate distributed flexibility that is available for offering to the day-ahead energy market by DSOs without jeopardizing the operational constraints of the distribution network. Further, the energy flexibility provided to power distribution systems by water treatment plants and battery electric bus charging infrastructures is modeled and optimized in [27,28].

Although DFRs can potentially provide both energy flexibility and regulation capacity, the technical literature lacks a comprehensive model that effectively captures and co-optimizes the flexibility of DFRs to deliver services in both energy and regulation markets, considering the operational constraints of distribution networks. When co-optimizing DFRs schedules in energy and regulation markets, it is critical to ensure that the limited capacity of DFRs is appropriately allocated to the services while maximizing DSO's profit in the markets. In addition, due to the power losses and operation constraints of distribution networks, energy flexibility and regulation capacity available at the DSO/ISO interface are not simply the summation of the distributed flexibility offered in distribution buses.

1.1. Contribution and paper structure

This paper proposes a comprehensive model to define, model and co-optimize the *deliverable energy flexibility* and *deliverable frequency regulation capacity* that a power distribution network with a given DFRs portfolio can offer to the day-ahead electricity markets. In the proposed model, distributed energy flexibility and regulation capacity are provided in distribution buses by flexible loads, distributed solar generation (DSG) units, and ES devices. The flexible loads are modeled by a novel queuing system that represents the aggregate behavior of a large population of distributed flexible loads in distribution buses, taking into account their type and service quality requirements. Further, DSG units and ES devices provide energy flexibility and regulation services through controllable inverters.

The *deliverable energy flexibility and regulation capacity* are defined as the aggregate flexibility at the DSO and ISO interface that is available for offering to the day-ahead energy and regulation markets without jeopardizing the operational constraints of distributed resources and distribution network. In order to co-optimize the deliverable energy flexibility and deliverable regulation capacity, a DSO flexibility scheduling model is proposed that co-optimizes the schedule of distributed resources in three different operating points for maximizing DSO's profit in the markets. The three operating points model the operation of flexible loads, DSG units, and ES devices in distribution systems for providing energy flexibility, as well as regulation up and down capacity in the markets. Each operating point represents a distinct energy transaction trajectory between the DSO and ISO, under which the schedule of distributed resources is co-optimized to provide energy flexibility, and regulation up and down capacity in the markets. In this regard, each operating point associated with a DFR represents a different power consumption or generation output profile based on DFRs constraints. The proposed model takes into account the interdependence between the DFR schedule in the three operating points, which enables the DSO to appropriately allocate the available distributed flexibility to different services without violating their operational constraints. The proposed model ensures the deliverability of the energy flexibility and regulation capacity in the markets by satisfying power flow constraints of distribution networks in all three operating points.

The remainder of this paper is organized as follows: the proposed models of deliverable energy flexibility and frequency regulation capacity are presented in Section 2. The proposed DSO flexibility scheduling model as well as DFRs models and their operation constraints are formulated in Section 3. The numerical results, conducted on the IEEE 33-bus distribution system, are presented in Section 4, and the conclusions are drawn in Section 5.

1.2. Notation

The notation used in the paper is defined as follows: we represent the power distribution network by a directed graph $G = (\mathcal{B}, \mathcal{L})$, where $\mathcal{B} = \{1, ..., B\}$ and $\mathcal{L} = \{ij | i, j \in \mathcal{B}, j \equiv j(i)\}$ respectively denote the set of buses and lines, and $j(i)$ shows the buses connected to bus i. In the power distribution network, which is considered to be radial, node $i = 1$ denotes the bus where the feeder is connected to the transmission substation, while the distribution buses are represented by set $\mathcal{B}^b = \{2, ..., B\}$. For each line $(ij) \in \mathcal{L}$, $y_{ij} = 1/z_{ij} = g_{ij} + ib_{ij}$ represents the complex admittance. In addition, the letters P, Q, C, D, E, A, O, F, R respectively represent the active and reactive power variables, the ES charge and discharge power variables, the ES stored energy variable, the flexible load arrivals, flexible loads queue backlog variable, the deliverable flexibility variable, and the regulation variable. The superscripts o, e, u, d, refer to the operating points O, E, U, D. Further the superscripts S, K, F respectively refer to the DSG units, ES devices, and flexible load variables. Finally, the subscripts t, c, i respectively denote the time intervals, flexible load clusters, and power distribution buses.

2. Deliverable energy flexibility and regulation capacity of distribution systems

In this section, we characterize the operating points where DSO seeks to simultaneously maximize its profit of providing services in day-ahead energy and regulation markets. The four operating points,

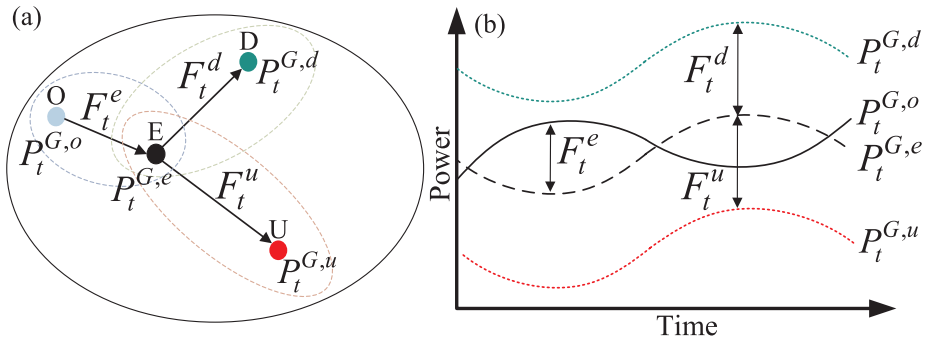

Fig. 1. (a) flexibility operating points, (b) flexibility trajectories.

utilized to define the deliverable energy flexibility and frequency regulation capacity of distribution networks, are shown in Fig. 1 and are described as follows:

– *Operating point O*, where DSO does not control DFRs and draws the energy trajectory $P_t^{G,o}$ from the ISO.
– *Operating point E*, where DSO controls DFRs to maximize its profit of selling energy reduction to the ISO. The energy transaction trajectory between the DSO and ISO in this point is denoted by $P_t^{G,e}$.
– *Operating point U*, where DSO controls DFRs to provide regulation up capacity such that its profit of providing the aggregate capacity to ISO is maximized. The energy transaction trajectory between the DSO and ISO in this point is denoted by $P_t^{G,u}$.
– *Operating point D*, where DSO controls DFRs to provide regulation down capacity such that its profit of providing the aggregate capacity to ISO is maximized. The energy transaction trajectory between the DSO and ISO in this point is denoted by $P_t^{G,d}$.

Deliverable energy flexibility at the DSO/ISO interface, denoted by F_t^e and shown in Fig. 1. (b), is defined as the difference of the energy transaction trajectory without and with controlling DFRs in the distribution network (i.e., operating points *O* and *E*), which is calculated as below:

$$F_t^e = (P_t^{G,o} - P_t^{G,e})\Delta t = F_t^{e^+} - F_t^{e^-}, \quad \forall\, t, \tag{1}$$

where $F_t^{e^+}$ and $F_t^{e^-}$ are positive variables that respectively represent the positive and negative parts of the deliverable energy flexibility. A positive value for F_t^e implies a reduction in the energy received by the DSO from ISO, and represents the available energy flexibility from the distribution network to be delivered to the day-ahead energy market. A negative energy flexibility value, on the other hand, denotes an increase in the energy received by the DSO from ISO.

Deliverable regulation up and down capacities at the DSO/ISO interface, denoted by positive variables F_t^u and F_t^d, are defined as the differences of the DSO and ISO energy transaction trajectory respectively between operating points *E* and *U*, and operating points *D* and *E* (see Fig. 1(b)), and are calculated as follows:

$$F_t^u = P_t^{G,e} - P_t^{G,u}, \quad \forall\, t, \tag{2}$$

$$F_t^d = P_t^{G,d} - P_t^{G,e}, \quad \forall\, t. \tag{3}$$

In summary, each operating point *E*, *U*, *D* and associated transition between two points (i.e., $O \to E$, $E \to U$, $E \to D$) represent a distinct energy transaction trajectory (e.g., a reduction or increase of the energy withdrawn from the transmission to the distribution system) between the DSO and ISO and therefore a unique service (i.e., energy flexibility, regulation up capacity, regulation down capacity) that results from this transaction. The energy transactions at the DSO/ISO interface change according to the different schedules of DFRs in the distribution buses. In this regard, each operating point associated with a DFR represents a different power consumption or generation output profile based on DFRs constraints.

Next, we introduce the DSO flexibility scheduling model that co-optimizes DFRs' schedules for providing energy flexibility and regulation up and down capacity in the markets.

3. DSO flexibility scheduling model

The structure of the proposed deliverable flexibility scheduling model is shown in Fig. 2. In Fig. 2, the DSO controls the distributed flexible loads (presented by load aggregators), solar units (interfaced by controllable inverters), and energy storage devices to co-optimize the deliverable energy and regulation up/down flexibility capacity defined in (1)–(3). The load aggregators are advanced communication systems that are owned by the DSO at distribution buses and exchange information between the DSO and flexible loads. The proposed model for co-optimizing the deliverable energy and regulation capacity of distribution networks is presented next.

3.1. Objective function

Consider a scheduling horizon $[0,\ T]$ that is divided into *N* intervals of the same length Δt, and $t \in \mathcal{T} = \{t_1,\ ...,t_n,\ ...,t_N\}$ refers to the starting points of intervals with $t_1 = 0$ and $t_N = T - \Delta t$. The objective function of the proposed model is to maximize DSO's profit from offering the energy flexibility and regulation up and down capacity to day-ahead energy and regulation markets over $\mathcal{T}$:

$$\max \sum_{t\in\mathcal{T}} F_t^{e^+}\pi_t^e - \sum_{t\in\mathcal{T}} F_t^{e^-}\pi_t^e + \sum_{t\in\mathcal{T}} F_t^u\pi_t^u + \sum_{t\in\mathcal{T}} F_t^d\pi_t^d, \tag{4}$$

where π_t^e, π_t^u, and π_t^d are the energy, regulation up and regulation down market prices at time *t*. The first term in (4) is the DSO's revenue from offering the positive deliverable energy flexibility (i.e., load reduction) to the day-ahead energy market, which is compensated at day-ahead wholesale energy price. The second term in (4) represents the cost of supplying the shifted flexible energy (i.e., the negative part of deliverable energy flexibility), which is purchased from ISO at day-ahead energy price. The third and fourth terms in (4) represent respectively the DSO's revenues from offering regulation up and down capacities in day-ahead regulation market.

The objective function (4) is constrained to the deliverable energy and regulation Eqs. (1)–(3), as well as the distribution network and DFRs constraints in three operating points *E*, *U*, and *D*. Hereafter, in order to simplify the formulation and avoid repetition, we refer to decision variables of the three operating points with superscript $x \in \{e,\ u,\ d\}$.

3.2. Flexible load aggregation constraints

The queuing model in [30] is expanded here to model the aggregate behavior of a large population of distributed flexible loads in distribution buses. In the proposed model, the load aggregators cluster flexible

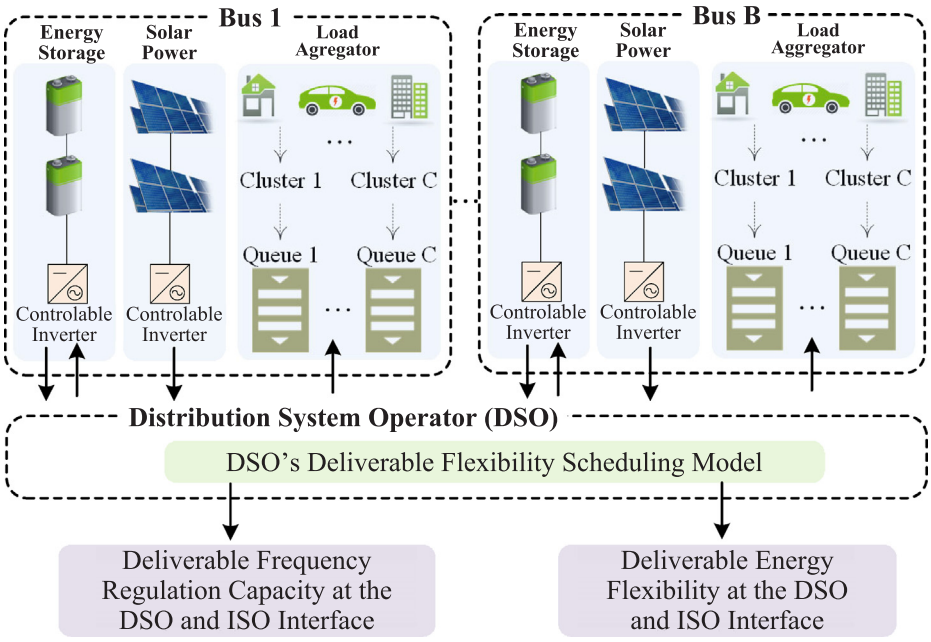

Fig. 2. The proposed DSO flexibility scheduling model.

loads in distribution buses based on their type (e.g., PEVs, dishwashers) and service quality requirements, and form multiple queues of flexible loads that represent their aggregate flexibility and service quality constraints in the system.

Let $A_{c,i,t}$ be the power consumption request of flexible loads received by load aggregator in bus $i \in \mathcal{B}^b$under cluster c in interval t. Also, let $P^{F,e}_{c,i,t}$ be the controlled flexible load (queue departure) decision variable, which is controlled by DSO to deliver energy flexibility in operating point E. Denoting the queue backlog of flexible loads in operating point E with $O^e_{c,i,t}$, state equation of the queuing system that logs the arrival and service of flexible loads is formulated as follows:

$$O^e_{c,i,t} = O^e_{c,i,t-\Delta t} + (A_{c,i,t} - P^{F,e}_{c,i,t})\Delta t, \qquad i \in \mathcal{B}^b, \forall\, c, \forall\, t. \tag{5}$$

While the deviation of flexible load consumption from $A_{c,i,t}$ to $P^{F,e}_{c,i,t}$ provides energy flexibility in operating point E, the controlled power consumption $P^{F,e}_{c,i,t}$ may be reduced to $P^{F,u}_{c,i,t}$ in (6) or increased to $P^{F,d}_{c,i,t}$ in (7), in order to respectively provide regulation up and down capacities $R^{F,u}_{c,i,t}$ and $R^{F,d}_{c,i,t}$ in operating points U and D. The queue backlog deviation due to provision of $R^{F,u}_{c,i,t}$ and $R^{F,d}_{c,i,t}$ is captured by deviation state Eq. (8), where $\Delta O_{c,i,t}$ denotes the deviation from the queue backlog $O^e_{c,i,t}$ in operating point E.

$$P^{F,u}_{c,i,t} = P^{F,e}_{c,i,t} - R^{F,u}_{c,i,t}, \qquad i \in \mathcal{B}^b, \forall\, c, \forall\, t, \tag{6}$$

$$P^{F,d}_{c,i,t} = P^{F,e}_{c,i,t} + R^{F,d}_{c,i,t}, \qquad i \in \mathcal{B}^b, \forall\, c, \forall\, t, \tag{7}$$

$$\Delta O_{c,i,t} = \Delta O_{c,i,t-\Delta t} + (R^{F,u}_{c,i,t} - R^{F,d}_{c,i,t})\Delta t, \; i \in \mathcal{B}^b, \forall\, c, \forall\, t. \tag{8}$$

The regulation up and down capacities provided by flexible loads are constrained respectively to five-min ramp rate limits $RR^{F,d}_c$ and $RR^{F,u}_c$ in (9) and (10). In addition, the controlled flexible load variables in operating point D are limited in (11) to their maximum electricity consumption values. Introducing binary variable $I^F_{c,i,t}$ in (9) and (10) prevents simultaneous offering of regulation up and down capacities.

$$0 \leqslant R^{F,u}_{c,i,t} \leqslant RR^{F,d}_c I^F_{c,i,t}, \forall\, c, \forall\, t, i \in \mathcal{B}^b, \tag{9}$$

$$0 \leqslant R^{F,d}_{c,i,t} \leqslant RR^{F,u}_c (1 - I^F_{c,i,t}), \forall\, c, \forall\, t, i \in \mathcal{B}^b, \tag{10}$$

$$0 \leqslant P^{F,d}_{c,i,t} \leqslant \overline{P^F_c}, \forall\, c, \forall\, t, i \in \mathcal{B}^b. \tag{11}$$

The proposed queuing model facilitates imposing *delay-based* and *deadline-based* service quality constraints of flexible loads, while scheduling the energy flexibility and regulation up and down capacities. The *delay-based constraint* (12) imposes maximum delay time $\tau_{c,i}$ on serving flexible loads, which requires that the cumulative energy consumption associated with the flexible load consumption request received until $t - \tau_{c,i}$ be less than or equal to the cumulative energy served until t [30]:

$$\sum_{t'=t_1}^{t-\tau_{c,i}} A_{c,i,t'}\Delta t \leqslant \sum_{t'=t_1}^{t} P^{F,e}_{c,i,t'}\Delta t, \;\; \forall\, c, t, i \in \mathcal{B}^b. \tag{12}$$

Adding and subtracting $\sum_{t'=t-\tau_{c,i}+\Delta t}^{t} A_{c,i,t'}\Delta t$ to left-hand-side of (12), and substituting $O^e_{c,i,t}$ from (5), we have:

$$0 \leqslant O^e_{c,i,t} \leqslant \overline{O^e_{c,i,t}}, \quad \forall\, c, t, i \in \mathcal{B}^b, \tag{13}$$

where, $\overline{O^e_{c,i,t}}$ is upper limit of the queue backlog defined as:

$$\overline{O^e_{c,i,t}} = \begin{cases} \sum_{t'=t-\tau_{c,i}+\Delta t}^{t} A_{c,i,t'}\Delta t & t \in \mathcal{T} - \{t_N\}, \\ 0 & t = t_N. \end{cases} \tag{14}$$

Constraints (13) and (14) specify that in order for DSO to be able to serve the consumption requests in delay time $\tau_{c,i}$, the queue backlog in interval t should not exceed the total consumption requests received from $\tau_{c,i}$ interval ago. Further, the queue backlog should be empty at the end of the scheduling horizon to make sure that all energy requested is served.

In addition, the queue backlog variable $O^e_{c,i,t}$in operating point E plus the queue deviation variable $\Delta O_{c,i,t}$should also respect the delay-based service quality constraint:

$$0 \leqslant O^e_{c,i,t} + \Delta O_{c,i,t} \leqslant \overline{O^e_{c,i,t}}, \quad \forall\, c, t, i \in \mathcal{B}^b. \tag{15}$$

The *deadline-based constraints* (16) and (17) ensure that flexible loads would be served before a given deadline time $t^D_{c,i}$, which requires the queue backlog to be empty at the deadline.

$$O^e_{c,i,t} = 0, \quad t = t^D_{c,i}, \;\; \forall\, c, i \in \mathcal{B}^b, \tag{16}$$

$$O^e_{c,i,t} + \Delta O_{c,i,t} = 0, \quad t = t^D_{c,i}, \;\; \forall\, c, i \in \mathcal{B}^b. \tag{17}$$

3.3. Energy Storage Constraints

Let $C^x_{k,t}$, $D^x_{k,t}$ and $E^x_{k,t}$ be positive variables respectively representing the active charging and discharging power, and the stored energy of ES k at t in operation point $x \in \{e, u, d\}$, and $Q^{K,x}_{k,t}$ be a free variable representing the ES reactive power. The ES state equation is formulated in (18), where η^C_k and η^D_k are the charging and discharging efficiencies. The charging, discharging and apparent powers of ES are confined in (19)–(21) to the rated values $\overline{C_k}$, $\overline{D_k}$, and $\overline{S^K_k}$, where binary variable $I^K_{k,t}$ in 19 and 20 eliminates the possibility of simultaneous charge and discharge. The ES stored energy is constrained to the energy capacity limits $\underline{E_k}$ and $\overline{E_k}$, and the initial ES energy is set to E^{init}_k in (23).

$$E^x_{k,t} = E^x_{k,t-\Delta t} + \left(\eta^C_k C^x_{k,t} - \frac{1}{\eta^D_k} D^x_{k,t}\right)\Delta t, \forall\, x, \forall\, k, \forall\, t, \tag{18}$$

$$C^x_{k,t} \leqslant \overline{C_k} I^K_{k,t}, \forall\, x, \forall\, k, \forall\, t, \tag{19}$$

$$D^x_{k,t} \leqslant \overline{D_k}(1 - I^K_{k,t}), \forall\, x, \forall\, k, \forall\, t, \tag{20}$$

$$(C^x_{k,t} + D^x_{k,t})^2 + (Q^{K,x}_{k,t})^2 \leqslant \overline{S^K_k}^2, \forall\, x, \forall\, k, \forall\, t, \tag{21}$$

$$\underline{E_k} \leqslant E^x_{e,t} \leqslant \overline{E_k}, \forall\, x, \forall\, k, \forall\, t, \tag{22}$$

$$E^x_{k,0} = E^{init}_k, \forall\, x, \forall\, k. \tag{23}$$

The ES charging power $C^e_{k,t}$ in operating point E may be reduced to $C^u_{k,t}$ in (24) or increased to $C^d_{k,t}$ in (25) in order to respectively provide regulation up and down capacities $R^{C,u}_{k,t}$ and $R^{C,d}_{k,t}$ in operating points U and D. In addition, ES discharging power $D^e_{k,t}$ in operating point E may be increased to $D^u_{k,t}$ in (26) or reduced to $D^d_{k,t}$ in (27) in order to respectively provide regulation up and down capacities $R^{D,u}_{k,t}$ and $R^{D,d}_{k,t}$ in operating points U and D. The ES regulation up and down capacities in charge and discharge states are constrained to the five-min ramp rate limits in (28)–(31).

$$C^u_{k,t} = C^e_{k,t} - R^{C,u}_{k,t}, \forall\, k, \forall\, t, \tag{24}$$

$$C^d_{k,t} = C^e_{k,t} + R^{C,d}_{k,t}, \forall\, k, \forall\, t, \tag{25}$$

$$D^u_{k,t} = D^e_{k,t} + R^{D,u}_{k,t}, \forall\, k, \forall\, t, \tag{26}$$

$$D^d_{k,t} = D^e_{k,t} - R^{D,d}_{k,t}, \forall\, k, \forall\, t, \tag{27}$$

$$0 \leqslant R^{C,u}_{k,t} \leqslant RR^{C,d}_k, \forall\, k, \forall\, t, \tag{28}$$

$$0 \leqslant R^{C,d}_{k,t} \leqslant RR^{C,u}_k, \forall\, k, \forall\, t, \tag{29}$$

$$0 \leqslant R^{D,u}_{k,t} \leqslant RR^{D,u}_k, \forall\, k, \forall\, t, \tag{30}$$

$$0 \leqslant R^{D,d}_{k,t} \leqslant RR^{D,d}_k, \forall\, k, \forall\, t. \tag{31}$$

3.4. Distributed solar generation with controllable inverter

Let $P^{S,x}_{s,t}$ and $Q^{S,x}_{s,t}$ be respectively the active and reactive powers of DSG unit s in operating point $x \in \{e, u, d\}$ at t. The active and apparent power of DSG units are respectively limited to the forecasted solar generation $\overline{P}^S_{s,t}$ in (32), and to the rated apparent power of the inverter $\overline{S}^S_s$ in (33). In addition, the power factor of DSG units is maintained above the minimum allowable power factor $\underline{PF_s}$ in (34).

$$0 \leqslant P^{S,x}_{s,t} \leqslant \overline{P^S_{s,t}}, \forall\, x, \forall\, s, \forall\, t, \tag{32}$$

$$P^{S,x2}_{s,t} + Q^{S,x2}_{s,t} \leqslant \overline{S^S}^2, \forall\, x, \forall\, s, \forall\, t, \tag{33}$$

$$\underline{PF_s} \leqslant \frac{P^{S,x}_{s,t}}{\sqrt{Q^{S,x2}_{s,t} + P^{S,x2}_{s,t}}}, \forall\, x, \forall\, s, \forall\, t. \tag{34}$$

The active power generation $P^{S,e}_{s,t}$ in operating point E may be increased to $P^{S,u}_{s,t}$ in (35) or reduced to $P^{S,d}_{s,t}$ in (36) in order to respectively provide regulation up and down capacities $R^{S,u}_{s,t}$ and $R^{S,d}_{s,t}$ in operating points U and D. In addition, the regulation up and down capacities of DSG units are limited to the associated five-min ramp rate limits in (37) and (38).

$$P^{S,u}_{s,t} = P^{S,e}_{s,t} + R^{S,u}_{s,t}, \forall\, s, \forall\, t, \tag{35}$$

$$P^{S,d}_{s,t} = P^{S,e}_{s,t} - R^{S,d}_{s,t}, \forall\, s, \forall\, t, \tag{36}$$

$$0 \leqslant R^{S,u}_{s,t} \leqslant RR^{S,u}_s, \forall\, s, \forall\, t, \tag{37}$$

$$0 \leqslant R^{S,d}_{s,t} \leqslant RR^{S,d}_s, \forall\, s, \forall\, t. \tag{38}$$

3.5. Distribution network constraints

Let $(P^{G,x}_t + \mathrm{i}Q^{G,x}_t)$ be the complex power flowing from the upstream transmission network to supply the distribution network and $(P^{L,x}_{ij,t} + \mathrm{i}Q^{L,x}_{ij,t})$ be the complex power flow of distribution lines in operating point $x \in \{e, u, d\}$ and interval t. Let also $(P^I_{i,t} + \mathrm{i}Q^I_{i,t})$ be the complex power of inflexible loads located in bus $i \in \mathcal{B}^b$ in interval t. The full AC power flow model is adopted to model distribution network operation with flexible loads, ES systems and DSG units as follows:

$$P^{G,x}_t = \sum_{1j \in \mathcal{L}} P^{L,x}_{1j,t}, \forall\, x, \forall\, t, \tag{39}$$

$$Q^{G,x}_t = \sum_{1j \in \mathcal{L}} Q^{L,x}_{1j,t}, \forall\, x, \forall\, t, \tag{40}$$

$$\sum_{s \in \mathcal{S}_i} P^{S,x}_{s,t} - P^I_{i,t} - \sum_{c \in C} P^{F,x}_{c,i,t} + \sum_{k \in \mathcal{K}_i} \left(D^x_{k,t} - C^x_{k,t}\right) = \sum_{ij \in \mathcal{L}} P^{L,x}_{ij,t}, \forall\, x, \forall\, t, i \in \mathcal{B}^b, \tag{41}$$

$$\sum_{s \in \mathcal{S}_i} Q^{S,x}_{s,t} - Q^I_{i,t} - \sum_{c \in C} Q^{F,x}_{c,i,t} + \sum_{k \in \mathcal{K}_i} Q^{K,x}_{k,t} = \sum_{ij \in \mathcal{L}} Q^{L,x}_{ij,t}, \forall\, x, \forall\, t, i \in \mathcal{B}^b, \tag{42}$$

$$P^{L,x}_{ij,t} = V^x_{i,t}{}^2 g_{ij} - V^x_{i,t} V^x_{j,t} g_{ij} \cos(\theta^x_{i,t} - \theta^x_{j,t}) - V^x_{i,t} V^x_{j,t} b_{ij} \sin(\theta^x_{i,t} - \theta^x_{j,t}), \forall\, x, \forall\, t, (ij) \in \mathcal{L}, \tag{43}$$

$$Q^{L,x}_{ij,t} = -V^x_{i,t}{}^2 b_{ij} + V^x_{i,t} V^x_{j,t} b_{ij} \cos(\theta^x_{i,t} - \theta^x_{j,t}), - V^x_{i,t} V^x_{j,t} g_{ij} \sin(\theta_{i,t} - \theta_{j,t}), \forall\, x, \forall\, t, (ij) \in \mathcal{L}, \tag{44}$$

$$P^{L,x2}_{ij,t} + Q^{L,x2}_{ij,t} \leqslant \overline{S^L_{ij}}^2, \forall\, x, \forall\, t, (ij) \in \mathcal{L}, \tag{45}$$

$$\underline{V_i} \leqslant V^x_{i,t} \leqslant \overline{V_i}, \forall\, x, \forall\, t, i \in \mathcal{B}^b, \tag{46}$$

$$\underline{\theta_i} \leqslant \theta^x_{i,t} \leqslant \overline{\theta_i}, \forall\, x, \forall\, t, i \in \mathcal{B}^b, \tag{47}$$

$$V^x_{1,t} = 1, \;\; \theta^x_{1,t} = 0, \forall\, x, \forall\, t. \tag{48}$$

The active and reactive power balance constraints in the substation bus are formulated in (39) and (40). The active and reactive power balance constraints in distribution buses that integrate flexible loads, ES and DSG units are modeled in (41) and (42). Active and reactive line power flows, which appear at the right-hand-sides of (39)–(42), are defined respectively in (43) and (44). The apparent power flow of transmission lines, and voltage magnitudes and phase angles of distribution buses are constrained to their respective limits $\overline{S^L_{ij}}$, $\underline{V_i}$, $\overline{V_i}$, $\underline{\theta_i}$, and $\overline{\theta_i}$ in (45)–(47). Also, voltage magnitude and phase angle of the substation bus are respectively set to 1 and 0 in (48).

In summary, the proposed DSO's deliverable flexibility scheduling model is formulated as a mixed integer nonlinear programming problem as follows:

$$\begin{aligned} &\max \quad (4) \\ &\text{s. t.} \quad (1) - (3), (5) - (48). \end{aligned} \tag{49}$$

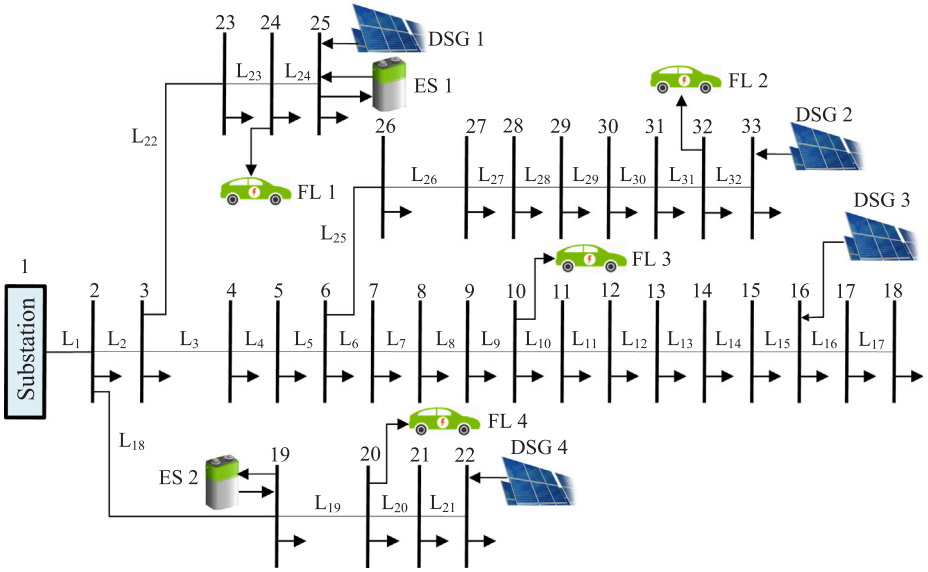

Fig. 3. The 33-bus test distribution system.

4. Numerical study

The proposed DSO flexibility scheduling model is implemented on the 33-bus distribution test system [31], shown in Fig. 3. The system is served by the upstream transmission network, as well as by four DSG units connected to buses 16, 22, 25 and 33 through controllable inverters.

The California Independent System Operator (CAISO) hourly load data for March 29–30, 2017 are scaled down to the test system's active and reactive peak loads of 3,715 kW and 2,300 kVAr, shown in Fig. 4, and used in the simulations. The CAISO's active solar power profile of the same period is scaled down to the inverters' rated active power output of 200 kW, representing the available forecasted solar power profile. Further, the CAISO's energy and frequency regulation prices of the same days are utilized in the simulations. Two ES units with energy and power ratings of 1500 kWh and 400 kW respectively, and charge and discharge efficiency of 85% are connected to buses 19 and 25 via controllable bi-directional inverters. The initial energy storage volume of the ES devices is set to 300 kWh. In addition, the minimum power factor for the solar inverters is set to 0.85 [32]. The upper and lower limits of the voltage magnitude at each distribution bus are set to 0.9 p.u. and 1.05 p.u., respectively.

Four load aggregators in buses 10, 20, 24 and 32 aggregate three types of PEV chargers (home, workplace and public) as flexible loads. The PEV charging load data for home, workplace, and public chargers for the city of Los Angeles are used in the simulations [33], where their peaks are scaled to 20% of the minimum active load of each bus. It is assumed that the home PEV load is served immediately from hour 8 to 16, and the PEV charge control is allowed by the customers after hour 16. For all PEV chargers, a single deadline is imposed at the hour 8 am of the next day. We also impose a delay constraint of two hours on the public PEV charging.

The numerical results are provided for four study cases. Case 0 simulates the operating point O where the DSO's operation goal is to supply the load of the system at the minimum cost, where DFRs are not optimized. The energy transaction at DSO/ISO interface in operating point O, $P_t^{G,o}$, is calculated from the solution of Case 0, which is then used in (1) for Cases 1 to 3. In Case 1, DFRs are utilized to only offer energy flexibility to day-ahead market. In Case 2, both energy flexibility and regulation capacity are co-optimized to offer to day-ahead market. Case 3 is similar to Case 2 without considering the distribution network's power flow constraints.

In order to cover the full decision space of the DSO flexibility scheduling model that includes the horizon for which the intertemporal service quality constraints of flexible loads are defined, the model is

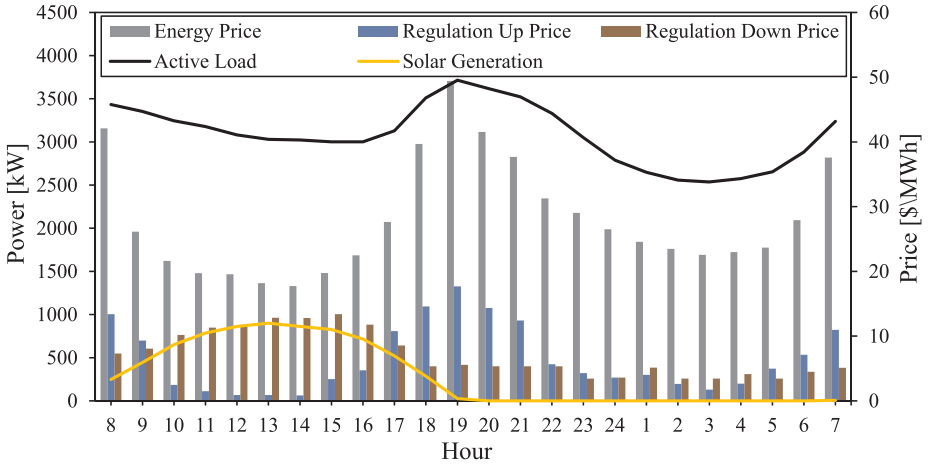

Fig. 4. Load, solar power, and energy and regulation up and down prices.

Table 1
DSO revenue, cost and profit components.

Cases	Energy Flexibility Revenue ($)	Energy Flexibility Cost ($)	Frequency Regulation Up Profit ($)	Frequency Regulation Down Profit ($)	Total Profit ($)
Case 1	754.7	37.9	0	0	716.8
Case 2	633.9	20.4	240.9	306.6	1,161.0
Case 3	770.3	11.4	342.7	372.3	1,473.9

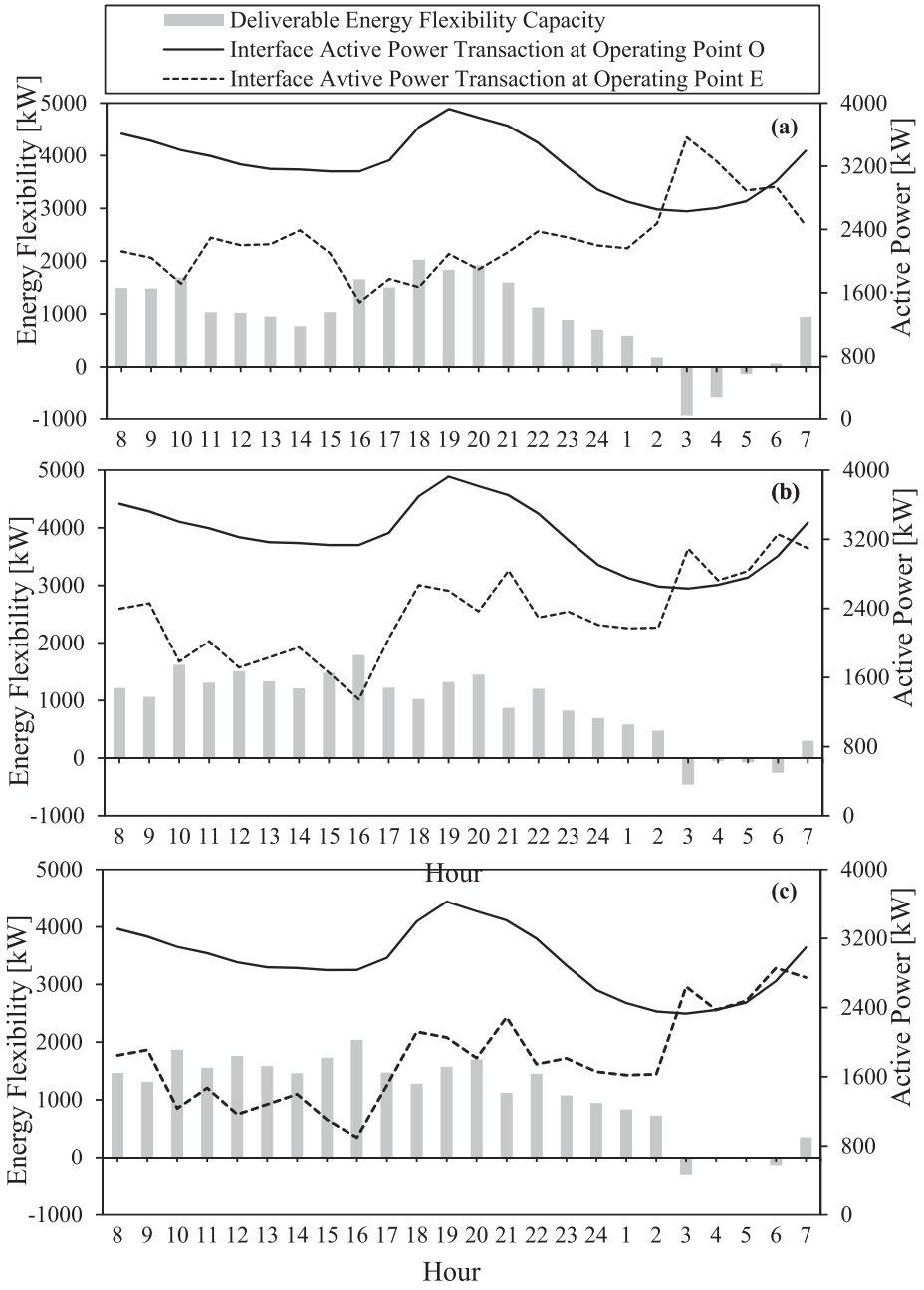

Fig. 5. DSO deliverable energy flexibility and active power transaction at the DSO/ISO interface: (a) Case 1, (b) Case 2, (c) Case 3.

solved for a scheduling horizon that extends from and utilizes the CAISO load and solar data of 8am, March 29, 2017 to 7am, March 30, 2017. The proposed MINLP model is solved using the BONMIN solver for Cases 0–3 on a desktop computer with a 4.0-GHz i7 processor and 32 GB of RAM, and results are presented next. Although, due to problem non-convexity, in theory, generic NLP solvers provide an (at least local) optimal solution on feasible problems, in practice, they most often provide the global optimum [29].

4.1. Results

4.1.1. DSO profit

The daily revenue, cost, and profit of DSO from offering the deliverable energy and regulation up/down capacity in day-ahead markets

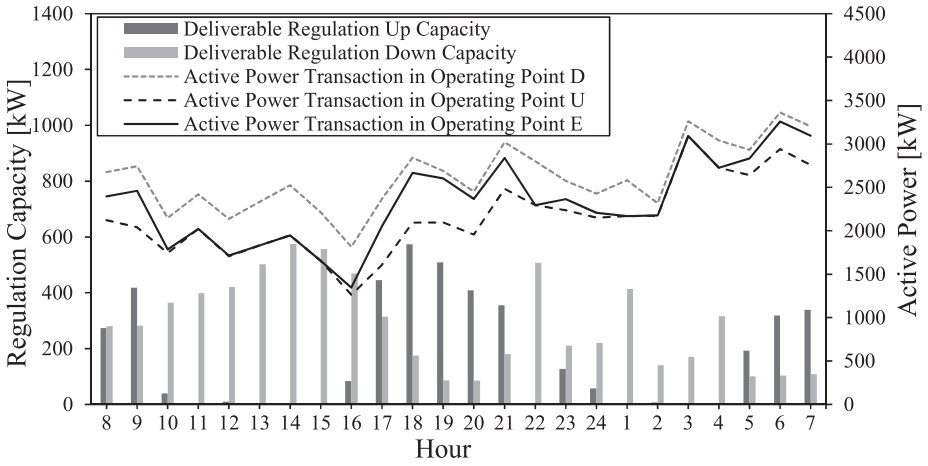

Fig. 6. DSO deliverable regulation capacity – Case 2.

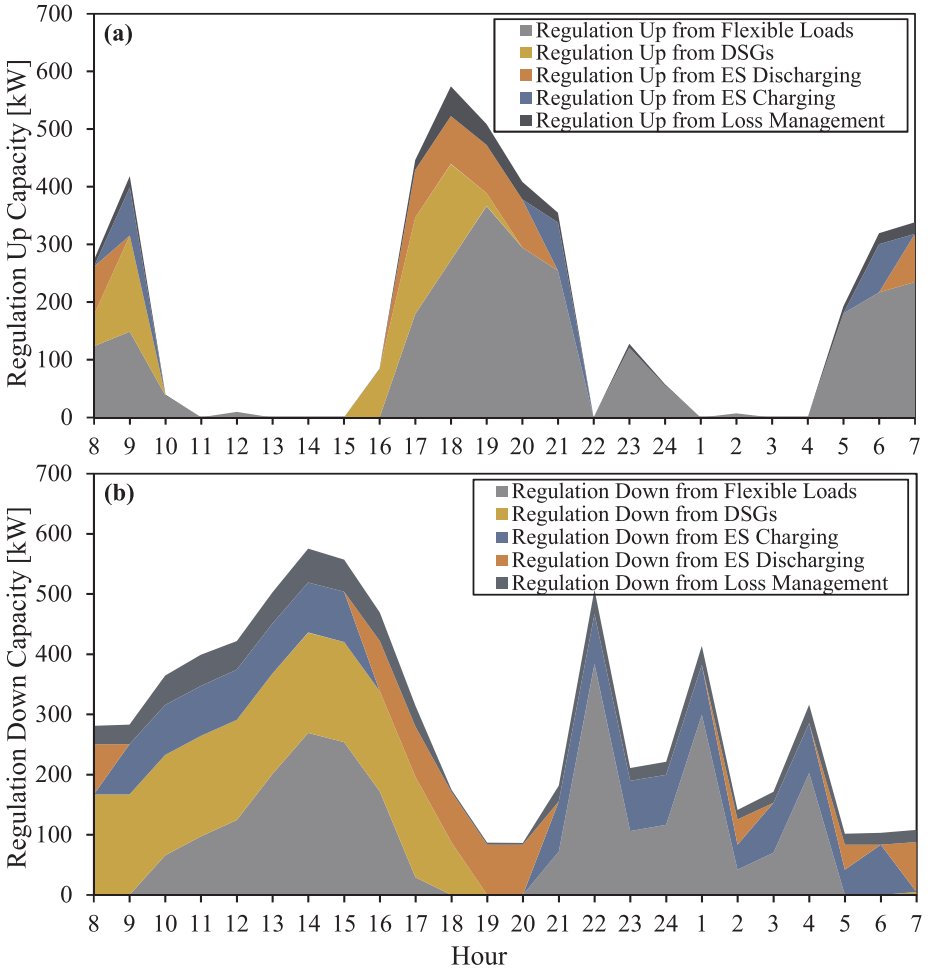

Fig. 7. Regulation (a) up and (b) down capacity.

are provided in Table 1. In Case 1, where DFRs are scheduled to offer their flexibility only in the day-ahead energy market, the DSO's revenues and costs are respectively $754.7 and $37.9, resulting in a total daily profit of $716.8. In Case 2, where DFRs are scheduled to offer their flexibility in both day-ahead energy and frequency regulation markets, the DSO's total profit is increased by 61.9% as compared to Case 1. In this case, the total daily DSO profit amounts to $1,161.0, out of which 52.8% and 47.2% result from offering energy flexibility and regulation capacity, respectively. In Case 3, where the power flow constraints are ignored, DSO's profit is increased by 26.9% as compared to Case 2. This result shows that ignoring power flow constraints leads to considerable overestimation of the DSO's energy flexibility and frequency regulation capacity, and the resulting profit in Case 3.

4.1.2. Deliverable energy flexibility

The DSO's deliverable energy flexibility schedule, as well as the active power transaction trajectory at the DSO/ISO interface in operating point *E* are shown in Fig. 5 for Cases 1 to 3. The positive and

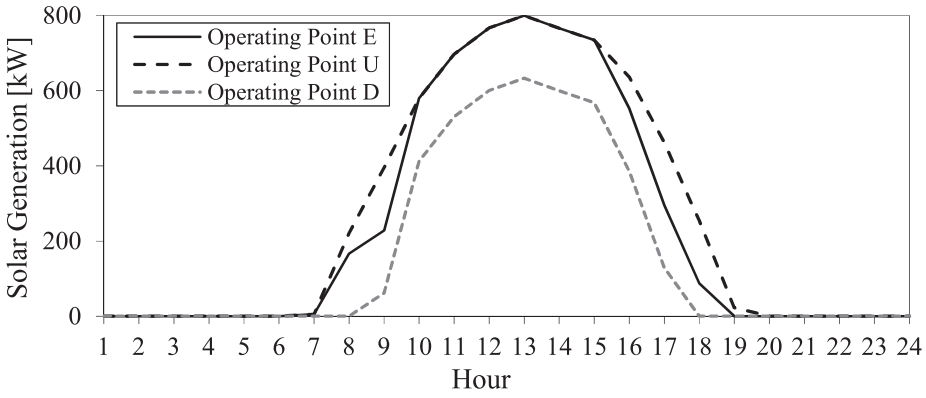

Fig. 8. Solar generation profile.

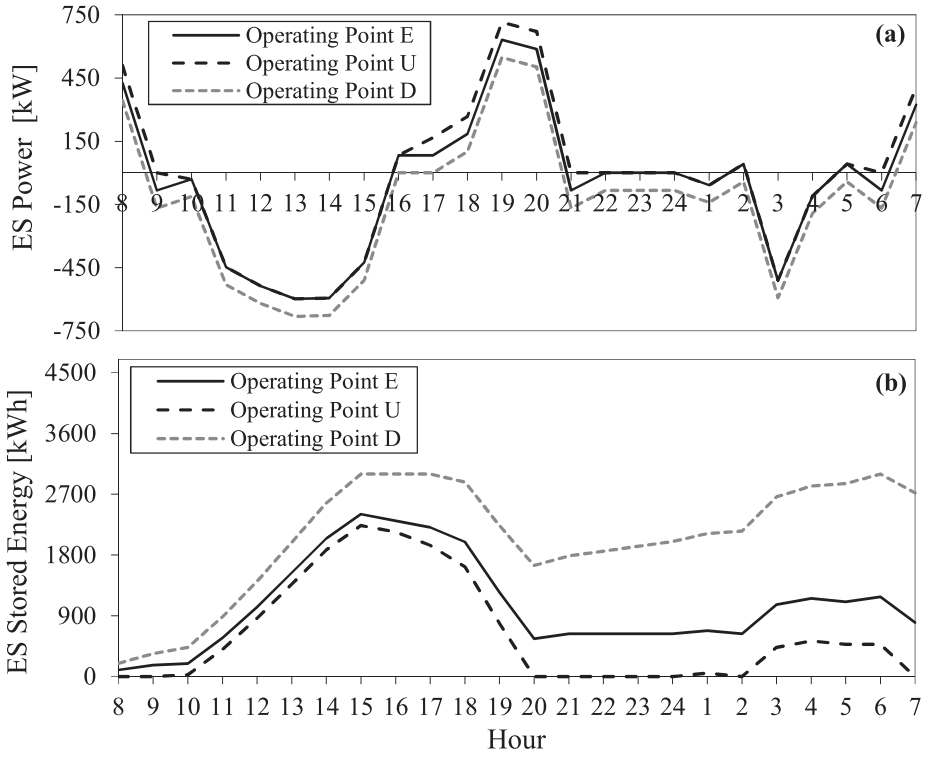

Fig. 9. (a) ES charge/discharge profile, (b) ES stored energy schedule.

negative values of the deliverable energy flexibility respectively represent the decrease and increase in the system's active power consumption as compared to Case 0. In Figs. 5, the DSO imports less active power from the upstream transmission network as compared to Case 0, since part of the network's active load is locally supplied by the DSG units. In addition, the flexible loads and ES devices are respectively queued and discharged during high energy price hours 8–10 and 16–21 in Case 1, which reduces the active power delivery from the upstream transmission network during these hours. In Fig. 5. (b), active power transaction trajectory in Case 2 differs from that of Case 1, indicating that a portion of DFRs capacity is reserved to be offered in the regulation up and down markets. As a result, the deliverable energy flexibility values are reduced in Case 2 as compared to Case 1. In Case 3, where the power flow constraints are ignored, the DSO offers more energy flexibility to the market in Fig. 5(c), since the power losses are zero and the operational constraints of the distribution network are ignored.

4.1.3. Deliverable regulation capacity

The DSO/ISO active power transaction trajectory in operating points *U* and *D*, and the resulting deliverable regulation capacity for Case 2 are shown in Fig. 6. In Fig. 6, the deliverable regulation up and down capacity follow the regulation up and down price profiles in Fig. 4. During the high regulation down prices in hours 10–16, the DSO utilizes DFRs to only schedule regulation down capacity. Similar trend is observed for regulation up capacity that is maximized during high regulation up price hours 17–21.

The contribution of individual DFRs in offering regulation capacity in Case 2 is shown in Fig. 7. In both Fig. 7(a) and (b), the flexible loads dominate in providing regulation up and down capacity. In both Fig. 7(a) and (b), a portion of regulation up and down capacity is provided through managing the active power losses of the network. More specifically, rescheduling DFRs for offering regulation up/down flexibility changes power flow in distribution lines, leading to a reduction/increase in the power losses of the system. This reduction or increase in power losses results in additional regulation up or down capacity in the DSO/ISO interface.

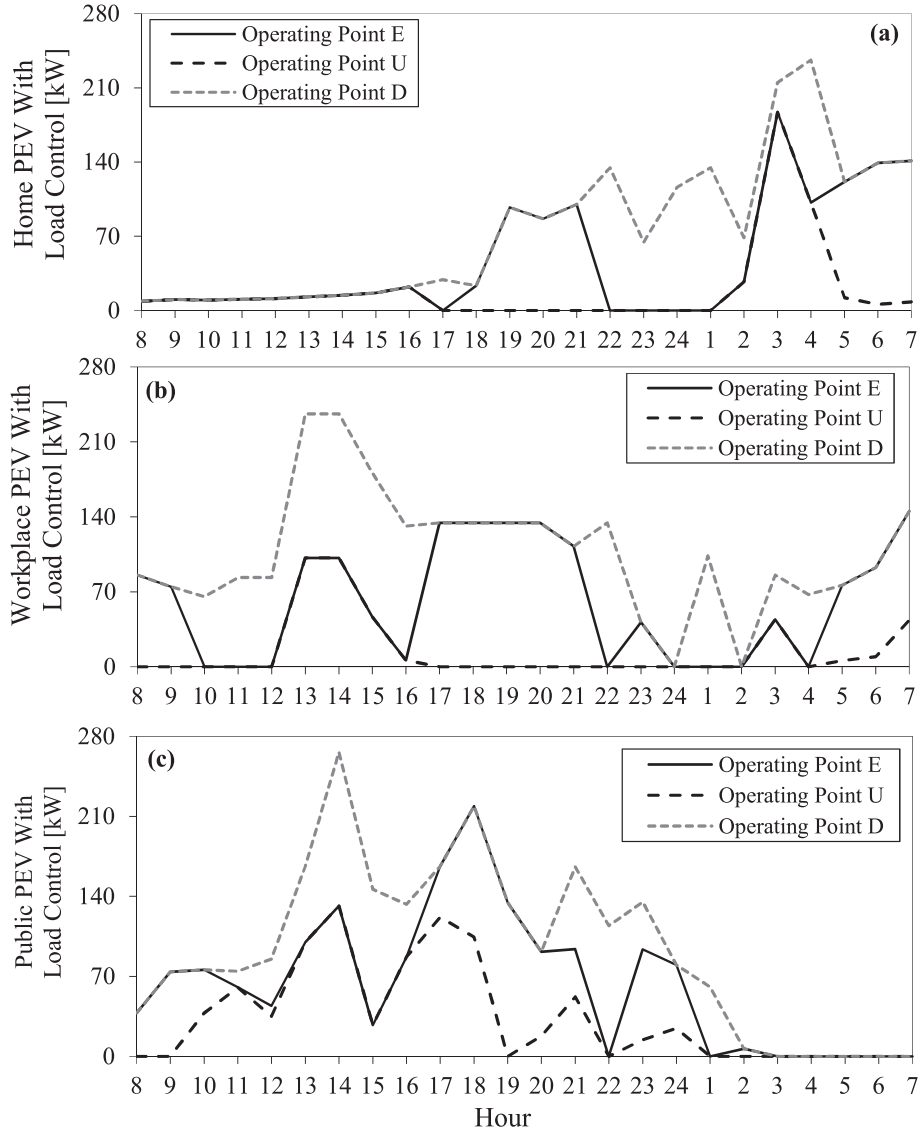

Fig. 10. (a) Home PEV load profile, (b) Workplace PEV load profile, (c) Public PEV load profile.

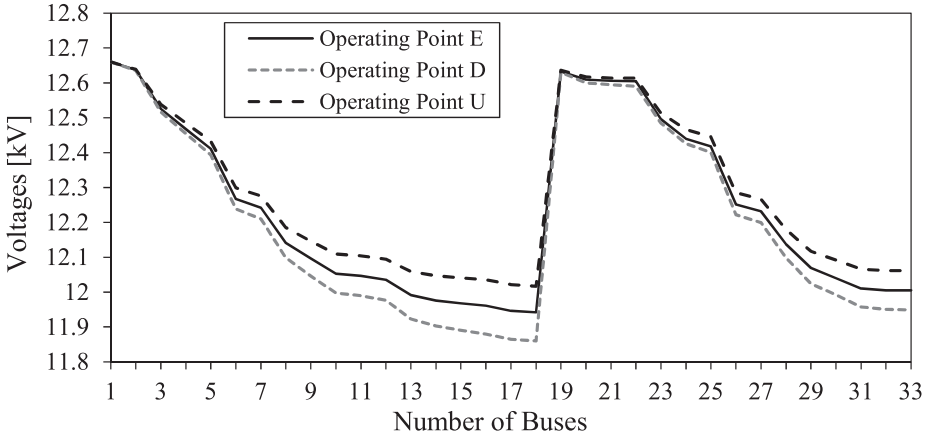

Fig. 11. DSO voltage profile.

4.1.4. Distributed flexibility resource schedule

DFRs schedule in operating points *E*, *U*, and *D* are displayed in Fig. 8–10. In Fig. 8, the DSG units provide regulation up capacity in hours 8–10 and 16–19 and regulation down flexibility in hours 9–18 by respectively increasing and decreasing the power output from the associated values in operating point *E*. In Fig. 9(a), ES is scheduled to provide regulation up and down capacity by deviating from the scheduled charge (negative) or discharge (positive) power values. The

proposed model ensures that the resulting deviation from the ES stored energy schedule, shown in Fig. 9(b), is within the capacity limits of ES, while ensuring the availability of stored energy to deliver the scheduled regulation up and down capacities.

The total controlled PEV load profiles in operating points *E*, *U* and *D* for the aggregated home, workplace and public clusters are shown in Fig. 10(a), (b) and (c). In Fig. 10(a), (b) and (c), the PEV charging loads are deviated from the ones in point *E* to provide regulation up and down capacities, while respecting the imposed service quality constraints.

4.1.5. Distribution bus voltages

Scheduling DFRs for offering regulation up/down capacity would increase and decrease the distribution bus voltages in operating points *U* and *D* as compared to the voltages in operating point *E*. The voltage in distribution buses in operating points *E*, *U* and *D*, averaged over the scheduling hours, is shown in Fig. 11. In Fig. 11, the largest voltage deviations are observed towards the end of the feeder in buses 11–18, 29–33 as these buses experience more voltage drop along the network, and therefore are more sensitive to active power flow fluctuations in distribution lines. Constraint (46) ensures that the voltage deviations would not violate the voltage limits, enabling the DSO to schedule the regulation capacity without violating the network constraints.

5. Conclusion

This paper proposes a comprehensive model to define and co-optimize the deliverable energy flexibility and frequency regulation capacity of power distribution networks, that is offered as the aggregate distributed flexibility to the day-ahead electricity market by DSOs. The distributed flexibility is provided by DFRs with different operation characteristics, including flexible loads, ES devices, and DSG units interfaced by controllable inverters. The proposed model incorporates three operating points for the distribution network and DFRs, which enable DSOs to control the transition of DFRs between the operating points in order to optimally allocate the available aggregate flexibility between the day-ahead energy and regulation up and down markets, while satisfying power distribution network constraints at all three operating points.

Simulation results demonstrated that the proposed model strategically allocates the available distributed flexibility to the energy and regulation up and down capacity offers so that the DSO's profit of participating in the markets is maximized. The proposed model ensures that the offered energy flexibility and regulation capacity can be reliably delivered at the DSO/ISO interface without jeopardizing the operating constraints of the distribution network and flexibility resources. Future works include considering the uncertainty of distributed flexible loads and solar power and developing a stochastic flexibility scheduling model for DSOs. In addition, the proposed DSO flexibility scheduling problem may be expanded to take into account the unbalanced three-phase operating condition in distribution systems.

Declaration of Competing Interest

None.

Appendix A. Supplementary material

Supplementary data associated with this article can be found, in the online version, at https://doi.org/10.1016/j.ijepes.2020.106219.

References

[1] Cochran J, Miller M, Zinaman O, Milligan M, Arent D, Palmintier B, et al. Flexibility in 21st century power systems. National Renewable Energy Lab.(NREL), Golden, CO (United States), Tech Rep; 2014.

[2] Ulbig A, Andersson G. Analyzing operational flexibility of electric power systems. Int J Electr Power Energy Syst 2015;72:155–64.

[3] Mohandes B, El Moursi MS, Hatziargyriou ND, El Khatib S. A review of power system flexibility with high penetration of renewables. IEEE Trans Power Syst 2019.

[4] Rahimi F, Mokhtari S. A new distribution system operator construct. Miineapolis USA: OATI; 2014.

[5] Parvania M, Fotuhi-Firuzabad M, Shahidehpour M. Iso's optimal strategies for scheduling the hourly demand response in day-ahead markets. Power Syst, IEEE Trans 2014;29(6):2636–45.

[6] Evangelopoulos VA, Georgilakis PS, Hatziargyriou ND. Optimal operation of smart distribution networks: a review of models, methods and future research. Electric Power Syst Res 2016;140:95–106.

[7] Parvania M, Fotuhi-Firuzabad M, Shahidehpour M. Optimal demand response aggregation in wholesale electricity markets. IEEE Trans Smart Grid 2013;4(4):1957–65.

[8] Arnold DB, Sankur MD, Negrete-Pincetic M, Callaway DS. Model-free optimal coordination of distributed energy resources for provisioning transmission-level services. IEEE Trans Power Syst 2018;33(1):817–28.

[9] Farrokhseresht M, Paterakis NG, Gibescu M, Slootweg J. Participation of a combined wind and storage unit in the day-ahead and local balancing markets. In: 2018 15th International conference on the European Energy Market (EEM). IEEE; 2018. p. 1–5.

[10] Dolan MJ, Davidson EM, Kockar I, Ault GW, McArthur SD. Distribution power flow management utilizing an online optimal power flow technique. IEEE Trans Power Syst 2012;27(2):790.

[11] Liu C, Chi F, Jin X, Mu Y, Jia H, Qi Y. A multi-level control strategy for transmission congestion relief based on the capability from active distribution network. In: Power system technology (POWERCON), 2014 international conference on. IEEE; 2014. p. 2000–6.

[12] Jin C, Tang J, Ghosh P. Optimizing electric vehicle charging with energy storage in the electricity market. IEEE Trans Smart Grid 2013;4(1):311–20.

[13] Vagropoulos SI, Kyriazidis DK, Bakirtzis AG. Real-time charging management framework for electric vehicle aggregators in a market environment. IEEE Trans Smart Grid 2016;7(2):948–57.

[14] Vayá MG, Andersson G. Optimal bidding strategy of a plug-in electric vehicle aggregator in day-ahead electricity markets under uncertainty. IEEE Trans Power Syst 2015;30(5):2375–85.

[15] Vayá MG, Andersson G. Self scheduling of plug-in electric vehicle aggregator to provide balancing services for wind power. IEEE Trans Sustain Energy 2016;7(2):886–99.

[16] Yao E, Wong VW, Schober R. Robust frequency regulation capacity scheduling algorithm for electric vehicles. IEEE Trans Smart Grid 2017;8(2):984–97.

[17] Bilgin E, Caramanis MC, Paschalidis IC, Cassandras CG. Provision of regulation service by smart buildings. IEEE Trans Smart Grid 2016;7(3):1683–93.

[18] Vrettos E, Oldewurtel F, Andersson G. Robust energy-constrained frequency reserves from aggregations of commercial buildings. IEEE Trans Power Syst 2016;31(6):4272–85.

[19] Farivar M, Neal R, Clarke C, Low S. Optimal inverter var control in distribution systems with high pv penetration. In: Power and energy society general meeting, 2012 IEEE. IEEE; 2012. p. 1–7.

[20] Dall'Anese E, Dhople SV, Giannakis GB. Optimal dispatch of photovoltaic inverters in residential distribution systems. IEEE Trans Sustain Energy 2014;5(2):487–97.

[21] Dalhues S, Zhou Y, Pohl O, Rewald F, Erlemeyer F, Schmid D, et al. Research and practice of flexibility in distribution systems: A review. CSEE J Power Energy Syst 2019;5(3):285–94.

[22] Gonzalez DM, Hachenberger J, Hinker J, Rewald F, Häger U, Rehtanz C, Myrzik J. Determination of the time-dependent flexibility of active distribution networks to control their tso-dso interconnection power flow. In: 2018 Power Systems Computation Conference (PSCC). IEEE; 2018. p. 1–8.

[23] Silva J, Sumaili J, Bessa RJ, Seca L, Matos M, Miranda V. The challenges of estimating the impact of distributed energy resources flexibility on the tso/dso boundary node operating points. Comput Oper Res 2018;96:294–304.

[24] Ji H, Wang C, Li P, Song G, Yu H, Wu J. Quantified analysis method for operational flexibility of active distribution networks with high penetration of distributed generators. Appl Energy 2019;239:706–14.

[25] Laur A, Nieto-Martin J, Bunn DW, Vicente-Pastor A. Optimal procurement of flexibility services within electricity distribution networks. Eur J Oper Res 2018.

[26] Oikonomou K, Parvania M, Khatami R. Deliverable energy flexibility scheduling for active distribution networks. IEEE Trans Smart Grid 2020;11(1):655–64.

[27] Oikonomou K, Parvania M. Deploying water treatment energy flexibility in power distribution systems operation. In: 2020 IEEE Power & Energy Society Innovative Smart Grid Technologies Conference (ISGT). IEEE; 2020. p. 1–5.

[28] Bagherinezhad A, Palomino AD, Li B, Parvania M. Spatio-temporal electric bus charging optimization with transit network constraints. IEEE Trans Ind Appl 2020.

[29] Capitanescu F. Critical review of recent advances and further developments needed in ac optimal power flow. Electric Power Syst Res 2016;136:57–68.

[30] Khatami R, Heidarifar M, Parvania M, Khargonekar P. Scheduling and pricing of load flexibility in power systems. IEEE J Select Top Signal Process 2018;12(4):645–56.

[31] Baran ME, Wu FF. Network reconfiguration in distribution systems for loss reduction and load balancing. IEEE Trans Power Deliv 1989;4(2):1401–7.

[32] Stetz T, Künschner J, Braun M, Engel B. "Cost-optimal sizing of photovoltaic inverters–influence of new grid codes and cost reductions," in 25th European PV Solar Energy Conference and Exhibition. Valencia 2010;2(1):5022–4.

[33] Idaho National Lab. [Online]. Available: <https://avt.inl.gov/>.